

**HEAT MASS TRANSFER OF NANOFLUIDS FLOW WITH
ABSORPTION IN THE PRESENCE OF THERMAL RADIATION**

S.Y. Zayyanu, I.J. Uwanta and M.M. Hamza

Department of Mathematics
Usmanu Danfodiyo University
Sokoto, Sokoto, Nigeria

Received December 16, 2019

Abstract

This study investigates the effects of chemical absorption on Heat Mass transfer of nanofluids flow over an infinite vertical plate in the presence of thermal radiation and applied magnetic field. the fluid is assumed to be electrically conducting water based Cu-nanofluid. The Tiwari and Das model is used to model the nanofluid, whereas Rosseland approximation is used for thermal radiation effect. Solutions for time dependent velocity, temperature and concentration equations are obtained using Laplace transform technique. The physical quantities of engineering interest such as skin friction, Nusselt number and Sherwood number are also computed. The obtained analytical solutions satisfy all imposed initial and boundary conditions. The effect of various parameters controlling the physical situation is discussed with the aid of line graphs. During the course of computation, excellent result was found from various physical parameters embedded in the problem.

Keywords: Nanofluid, Chemical absorption, Thermal radiation, Heat transfer, Mass transfer.

List of Constants

C	Dimensionless Concentration
C_f	Skin friction coefficient
C_p	Specific heat capacity of fluid (J/KgK)
g	Acceleration due to gravity
Kr	Chemical reaction parameter
Ka	Chemical absorption parameter
K	Thermal conductivity
K^*	Rosseland mean absorption coefficient
M	Magnetic parameter
Nu	Nusselt number
Pr	Prandtl number
Q_o	Chemical absorption coefficient
Grc	Solutal grashof number
Grt	Thermal grashof number
q_r	Radiative heat flux
R	Radiation parameter
Sc	Schmidt number
Sh	Sherwood number
t	Dimensionless time
T	Dimensional temperature
θ	Dimensionless temperature
u^*	Dimensional velocity
u	Dimensionless velocity
t^*	Dimensional time
y^*	Cartesian coordinate along the plate
D_{nf}	Mass diffusion coefficient

K_o^* Chemical reaction coefficient

Greek Symbols

ν Kinematic viscosity
 μ_{nf} Dynamic viscosity($Kg / m^{-1}s^{-1}$)
 φ Nanoparticle volume fraction
 σ^* Stefan-Boltzmann constant
 σ Electric conductivity of fluid
 ρ Density
 β Thermal expansion coefficient
 q Laplace parameter

Subscript

f Based fluid
 s Solid nanoparticle
 w At the wall condition
 ∞ Far from the wall

1.0 Introduction

Recent advances in nanotechnology have allowed the development of a new category of fluids termed nanofluids. A nanofluid refers to the suspension of nanosize particles, which are suspended in the based fluid with low thermal conductivity, these particles also called nanoparticles, have a diameter of less than 100nm. The base fluid or dispersing medium can be aqueous or non-aqueous in nature. Nanofluids or so called smart fluids research has attracted considerable attention in recent years owing to their significance in engineering application and technology. The broad range of current and future applications have been given in the studies by, Wang and Mujumdar [1], Kakac and Pramuanjaroenkij [2], Eapen *et al.* [3] and Fan and Wang [4]. Recently, Sheikholeslami and gamji [5] studied the MHD effects on Nanofluid flow in a permeable channel. Kuznetsov and Nield [6] critically analyzed the natural convection flow of a Nanofluid past a vertical plate. The problem of transient MHD free convection flow of a Nanofluid over a rotating vertical plate is addressed by Hamad and Pop [7]. They solved the governing equations analytically using the perturbation method and found that, the inclusion of nanoparticles into the based fluid is capable of varying the flow pattern. Turkyilmazoglu [8] reported the exact solution for heat and mass transfer of magnetohydrodynamic flow of nanofluid. Further, Turkyilmazoglu and Pop [9] have examined the heat and mass transfer of unsteady natural convection flow of nanofluid past a vertical plate with thermal radiation. Das [10] discussed the

problem of free convection flow of nanofluid bounded by moving vertical plate with constant heat source and convective boundary condition in a rotating frame of reference. He found that, the skin friction coefficient increases with an increase in nanoparticle volume fraction. However, Sheikholeslami *et al.* [11] have presented the heat and mass transfer behavior of unsteady flow of Nanofluid between parallel plates in the presence of thermal radiation. They concluded that, the solutal boundary layer thickness increases with increase in radiation parameter. Giresha *et al.*[12] have studied the effect of nanoparticles on flow and heat transfer of dusty fluid. Das and Jana [13] studied the MHD flow past a moving vertical plate in the presence of thermal radiation using Laplace transform method for closed form expressions of flow fields, they found that, the sheer stress at the plate for Cu -water nanofluid is found to be lower. Heat transfer in flow of nanofluid with heat source/sink and an induced magnetic field is addressed by Giresha *et al.*[14]. The boundary layer in newtonian and porous media filled by nanofluids over fixed and moving boundaries have been studied by Mahdy and Elshehabey [15].

In many industrial and engineering applications, the heat and mass transfer is a consequence of buoyancy caused by thermal diffusion and chemical species, therefore, the study of heat and mass transfer is needed for improving many technologies such as polymer and ceramic production, food processing, gas production, geothermal reservoirs, thermal insulations and so on. The heat and mass transfer flow of nanofluids in the presence of magnetic field also find a variety of applications such as energy saving, reduction of production time and also a

greater quality of the final product. Heat and mass transfer under the influence of chemical reaction has also attracted considerable attention of many authors due to wide range of applications. In view of these, conjugate heat and mass transfer flow past a vertical permeable plate with thermal radiation and chemical reaction is investigated by Pal and Talukdar [16]. They found that, the thermal radiation and chemical reaction effect decrease the velocity and concentration profiles. Numerical investigation of heat and mass transfer of an electrically conducting fluid over a moving surface with first order chemical reaction is carried out by Chamkha [17]. Uwanta and Omokhuale [18] have analyzed the influence of radiation and chemical reaction effect on heat and mass transfer of a viscoelastic fluid in a mixed plane. Later, the combined effects of radiation and chemical reaction on the MHD free convection flow of an electrically conducting viscous fluid over an inclined plate have been studied by Ali *et al.*[19] and have obtained a closed form solution by employing Laplace transform technique. Fetecau *et al.*[20], studied natural convection flow of fractional nanofluids over an isothermal vertical plate.

Motivated by aforementioned studies, we intend to investigate/extend the study reported by Fetecau *et al.*[20], the effect of heat and mass transfer on natural convection flow over a vertical plate, the effects of chemical

absorption, chemical reaction are also considered, to best of our knowledge, this study has not been considered by any author, our interest here, is to obtain the closed form solution for the present problem by employing Laplace Transform technique, the basic partial differential equations are derived by using Boussinesq approximation and then are transformed to dimensionless equations using suitable non-dimensional parameters. The resultant equations have been solved analytically.

2.0 Mathematical Formulation and Solution

Consider the natural convection flow, heat and mass transfer of nanofluid, past an infinite vertical plate situated in the (x^*, z^*) -plane of a fixed Cartesian coordinate system $Ox^* y^* z^*$. The plate is at rest initially with constant ambient temperature and concentration T_∞ and C_∞ respectively, uniform transverse magnetic field of strength (β_0) and radiative heat flux (q_r) are applied perpendicular to the plate. It is assumed that the pressure gradient is neglected and the fluid is electrically conducting, water based nanofluid embedded with copper nanoparticles. Since the plate is infinite, all of the physical quantities describing the fluid motion are functions of y^* and t^* .

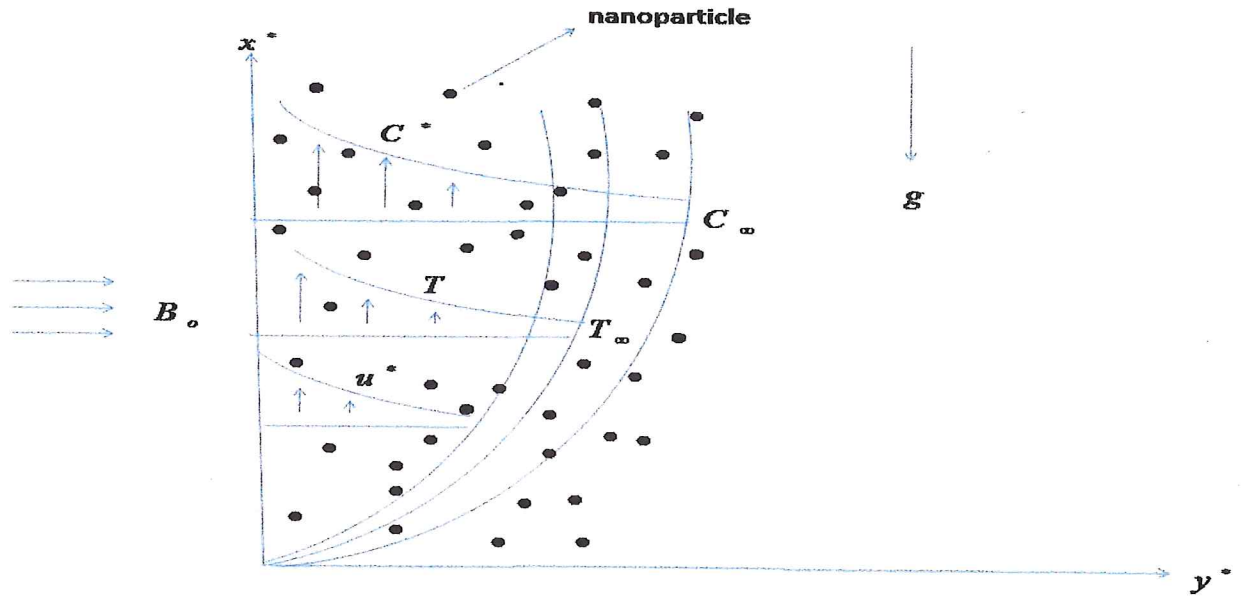


Fig.1: GEOMETRY OF THE PROBLEM

The thermophysical properties of copper (*Cu*) are given in table1 (Oztop and Abu-nada [22]).

Physical properties	base fluid	<i>Cu</i>
ρ (kg/m^3)	997.1	8933
C_p (J/kgK)	4179	385
K (W/mK)	0.613	401
$\beta_t \times 10^5$ (K^{-1})	21	1.67
$\beta_c \times 10^6$ (m^2/h)	298.2	3.05

φ	0.0	0.05
σ (s / m)	5.5×10^{-6}	59.6×10^6

TABLE 1: Thermophysical properties of copper (*Cu*)

Assuming small differences between the temperature $T(y^*, t^*)$ and the stream temperature T_∞ , and adopting the Rosseland approximation [5], the radiative heat flux $q_r(y^*, t^*)$ can be linearized to :

$$q_r(y^*, t^*) = -\frac{16\sigma^* T_\infty^3}{3K^*} \frac{\partial(y^*, t^*)}{\partial y^*} \quad (1)$$

Where σ^* is the Stefan-Boltzman constant and K^* is the mean absorption coefficient. In view of the above assumption and taking into account the nanofluid model proposed by Tiwari and Das [21], the governing equations can be written as:

$$\rho_{nf} \frac{\partial u^*}{\partial t^*} = \mu_{nf} \frac{\partial^2 u^*}{\partial y^{*2}} + g(\rho\beta)_{nf}(T - T_\infty) + g(\rho\beta)_{nf}(C^* - C_\infty) - \sigma_{nf} \beta_0^2 u^* \quad (2)$$

$$(\rho C p)_{nf} \frac{\partial T}{\partial t^*} = K_{nf} \left(1 + \frac{16\sigma^* T_\infty^3}{3K_{nf} K^*}\right) \frac{\partial^2 T}{\partial y^{*2}} + Q_0(C^* - C_\infty) \quad (3)$$

$$\frac{\partial C^*}{\partial t^*} = D_{nf} \frac{\partial^2 C^*}{\partial y^{*2}} - K_0^*(C^* - C_\infty) \quad (4)$$

In the above equations, $u^*(y^*, t^*)$ is the fluid velocity in the x^* direction, T_w is constant plate temperature ($T_w > T_\infty$ or $T_w < T_\infty$ corresponds to the Heated or cooled plate respectively), g is the acceleration due to gravity, σ_{nf} is the effective thermal conductivity, K_0^* the chemical reaction coefficient, D_{nf} is the diffusion coefficient and Q_0 is chemical absorption coefficient, ρ_{nf} is the density of the nanofluid, μ_{nf} is the dynamic viscosity of the nanofluid, β_{nf} is the thermal expansion coefficient of the nanofluid. The effective properties of nanofluid are given by the following co-relations (see Das and Jana [13]):

$$\begin{aligned} \mu_{nf} &= \frac{\mu_f}{(1-\varphi)^{2.5}} \quad , \quad \rho_{nf} = (1-\varphi)\rho_f + \varphi\rho_s \quad , \quad (\rho C_p)_{nf} = (1-\varphi)(\rho C_p)_f + \varphi(\rho C_p)_s \quad , \\ (\rho\beta)_{nf} &= (1-\varphi)(\rho\beta)_f + \varphi(\rho\beta)_s \quad , \quad \sigma_{nf} = \sigma_f \left(1 + \frac{3(\sigma-1)\varphi}{(\sigma+2) - (\sigma-1)\varphi} \right) \quad , \quad \sigma = \frac{\sigma_s}{\sigma_f} \quad , \\ \frac{K_{nf}}{K_f} &= \frac{K_s + 2K_f - 2\varphi(K_f - K_s)}{K_s + 2K_f + \varphi(K_f - K_s)} \end{aligned} \quad (5)$$

Where φ the volume fraction of nanoparticles, ρ_f and ρ_s are density of base fluid and nanoparticles respectively, C_{pf} and C_{ps} are specific heat of the base fluid and nanoparticles respectively, σ_f and σ_s are electrical conductivity of base fluid and nanoparticles correspondingly, β_f and β_s are thermal expansion coefficient of the

base fluid and nanoparticles respectively, K_f and K_s are thermal conductivity of base fluid and nanoparticles.

If no slipping exists between the fluid and the plate, the appropriate initial and boundary conditions are:

$$\begin{aligned} u^*(y^*, 0) = 0, T(y^*, 0) = T_\infty, C^*(y^*, 0) = C_\infty; y^* > 0 \\ u^*(0, t^*) = 0, T(0, t^*) = T_w, C^*(0, t^*) = C_w; t^* > 0 \\ u^*(y^*, t^*) = 0, T(y^*, t^*) = 0, C^*(y^*, t^*) = 0; y^* \rightarrow \infty \end{aligned} \quad (6)$$

The non-dimensional quantities introduced in the above equations are defined as :

$$\begin{aligned} y = \frac{y^*}{L}, \quad t = \frac{v_f t^*}{L^2}, \quad u = \frac{u^* L}{v_f}, \quad L^3 = \frac{v_f^2}{g\beta_f(T_w - T_\infty)}, \quad \theta = \frac{T - T_\infty}{T_w - T_\infty}, \quad C = \frac{C^* - C_\infty}{C_w - C_\infty}, \\ Kr = \frac{K_0^* L^2}{v_f}, \quad Sc = \frac{v_f}{D_{nf}}, \quad Pr = \frac{v_f}{K_f}, \quad Ra = \frac{16\sigma^* T_\infty^3}{3K^* K_f}, \quad Ka = \frac{L^2(C_w - C_\infty)}{v_f(T_w - T_\infty)(\rho Cp)_f}, \\ M^2 = \frac{\sigma_f \beta_0^2 L^2}{\rho_f v_f}, \quad G_{rc} = \frac{g\beta(C_w - C_\infty)}{v_f^2}, \quad G_{rt} = \frac{g\beta(T_w - T_\infty)}{v_f^2} \end{aligned} \quad (7)$$

On substituting these dimensionless variables into equations (2),(3) and (4) , one can get ;

$$\frac{\partial u}{\partial t} = \frac{1}{a_1} \frac{\partial^2 u}{\partial y^2} + a_2 \theta + a_3 C - a_5 u \quad (8)$$

$$\frac{\partial \theta}{\partial t} = \frac{1}{a_6} \frac{\partial^2 \theta}{\partial y^2} + a_7 C \quad (9)$$

$$\frac{\partial C}{\partial t} = \frac{1}{Sc} \frac{\partial^2 C}{\partial y^2} - KrC \quad (10)$$

With initial and boundary conditions

$$\begin{aligned} u(y, 0) = 0, \theta(y, 0) = 0, C(y, 0) = 0; y > 0 \\ u(0, t) = 0, \theta(0, t) = 1, C(0, t) = 1; t > 0 \\ u(y, t) = 0, \theta(y, t) = 0, C(y, t) = 0; y \rightarrow \infty \end{aligned} \quad (11)$$

By applying the Laplace Transform on both sides of equations (8) – (11), we have

$$\frac{d^2 \bar{u}}{dy^2} - (a_1(q + a_5))\bar{u} + a_1 a_2 \bar{\theta} + a_1 a_3 \bar{C} = 0 \quad (12)$$

$$\frac{d^2 \bar{\theta}}{dy^2} - a_6 q \bar{\theta} + a_6 a_7 \bar{C} = 0 \quad (13)$$

$$\frac{d^2 \bar{C}}{dy^2} - (Sc(q + Kr))\bar{C} = 0 \quad (14)$$

With corresponding initial and boundary conditions

$$\begin{aligned} \bar{u}(y, 0) = 0, \bar{\theta}(y, 0) = 0, \bar{C}(y, 0) = 0; y > 0 \\ \bar{u}(0, q) = 0, \bar{\theta}(0, q) = \frac{1}{q}, \bar{C}(0, q) = \frac{1}{q}; q > 0 \\ \bar{u}(y, t) = 0, \bar{\theta}(y, q) = 0, \bar{C}(y, q) = 0; y \rightarrow \infty \end{aligned} \quad (15)$$

Where $\bar{u} = \int_0^{\infty} u(y,t)l^{-qt} dt$, $\bar{\theta} = \int_0^{\infty} \theta(y,t)l^{-qt} dt$, $\bar{C} = \int_0^{\infty} C(y,t)l^{-qt} dt$ and $q > 0$. Now

by solving the above system ,one can have ;

$$\bar{C}(y,q) = \frac{1}{q} l^{-y\sqrt{(q+Kr)Sc}} \quad (16)$$

$$\bar{\theta}(y,q) = \frac{l^{-y\sqrt{a_6q}}}{q} + \frac{V_2}{V_1} \left(\frac{l^{-y\sqrt{(q+Kr)Sc}}}{q-V_1} - \frac{l^{-y\sqrt{(q+Kr)Sc}}}{q} - \frac{l^{-y\sqrt{a_6q}}}{q-V_1} + \frac{l^{-y\sqrt{a_6q}}}{q} \right) \quad (17)$$

$$\begin{aligned} \bar{u}(y,q) = & \frac{b_9 l^{-y\sqrt{(q+a_5)a_1}}}{q-V_4} + \frac{b_{10} l^{-y\sqrt{(q+a_5)a_1}}}{q} + \frac{b_{11} l^{-y\sqrt{a_1q}}}{q-V_4} + \frac{b_{12} l^{-y\sqrt{a_1q}}}{q} \\ & + \frac{b_4 l^{-y\sqrt{a_1q}}}{q-V_1} - \frac{b_{13} l^{-y\sqrt{(q+a_5)a_1}}}{q-V_1} + \frac{b_{14} l^{-y\sqrt{(q+Kr)Sc}}}{q+V_7} + \frac{b_6 l^{-y\sqrt{(q+Kr)Sc}}}{q+V_1} \\ & + \frac{b_{15} l^{-y\sqrt{(q+Kr)Sc}}}{q} + \frac{b_{16} l^{-y\sqrt{(q+a_5)a_1}}}{q+V_7} \end{aligned} \quad (18)$$

In order to determine, the flow fields in the time domain, by applying Inverse Laplace Transform on both sides of equations (16) - (18) , we get;

2.1 Velocity Equation

$$u(y,t) = b_9 I_1 + b_{10} I_2 + b_{11} I_3 + b_{12} I_4 + b_4 I_5 - b_{13} I_6 + b_{14} I_7 + b_6 I_8 + b_{15} I_9 + b_{16} I_{10} \quad (19)$$

2.2 Temperature Equation

$$\theta(y,t) = I_4 + c_2 I_{12} - c_2 I_9 - c_2 I_5 + c_2 I_4 \quad (20)$$

2.3 Concentration Equation

$$C(y,t) = I_9 \quad (21)$$

In order to determine the three entities of physical interest, namely the skin friction coefficient (C_f), Nusselt number (Nu) and Sherwood number (Sh), we use the relations;

2.4 Skin Friction (C_f)

The Skin friction coefficient at the plate $y=0$ is given by;

$$C_f = \frac{1}{(1-\phi)^{2.5}} \left. \frac{\partial u}{\partial t} \right|_{y=0} \quad (22)$$

$$\left. \frac{\partial u}{\partial t} \right|_{y=0} = \left(b_9 \frac{\partial I_1}{\partial y} + b_{10} \frac{\partial I_2}{\partial y} + b_{11} \frac{\partial I_3}{\partial y} + b_{12} \frac{\partial I_4}{\partial y} + b_4 \frac{\partial I_5}{\partial y} - b_{13} \frac{\partial I_6}{\partial y} + b_{14} \frac{\partial I_7}{\partial y} + b_6 \frac{\partial I_8}{\partial y} + b_{15} \frac{\partial I_9}{\partial y} + b_{16} \frac{\partial I_{10}}{\partial y} \right)_{y=0}$$

2.5 Nusselt Number (Nu)

The Nusselt number (Nu) at the plate $y=0$ is given by;

$$Nu = -\frac{K_{nf}}{K_f} \frac{\partial \theta}{\partial y} \Big|_{y=0} \quad (23)$$

$$\frac{\partial \theta}{\partial y} \Big|_{y=0} = \left(\frac{\partial I_4}{\partial y} + c_2 \frac{\partial I_{12}}{\partial y} - c_2 \frac{\partial I_9}{\partial y} - c_2 \frac{\partial I_5}{\partial y} + c_2 \frac{\partial I_4}{\partial y} \right) \Big|_{y=0}$$

2.6 Sherwood Number (Sh)

The Sherwood number (Sh) at the plate $y=0$ is given by;

$$Sh = -\frac{\partial I_9}{\partial y} \Big|_{y=0} \quad (24)$$

3.0 Results and Discussion

In the present study, the Laplace Transform technique has been employed to obtain the analytical expressions for Velocity, Temperature and Concentration profiles as well the Skin friction coefficient, Nusselt number and Sherwood number. In order to have the clear insight of the problem, a numerical computation has been carried out for different values of pertinent parameters. Throughout our numerical computation, the value of Prandtl number (Pr) has been taken to be 6.2 which corresponds to Cu water, Radiation parameter (R) has been taken as 1 (Fetecau *et al.*[20]), Schmidt number (Sc) is taken to be 0.6

which correspond to water vapor, other parameters are varied over the range which are listed in the figures legend.

Fig.2 is prepared to show that, an increase in chemical reaction parameter (Kr) decreases the concentration profile and vice-versa. The reason behind this is that, the number of solute molecules undergoing chemical reactions gets increased as chemical reaction parameter increases, which lead to decrease in concentration profile. While **Fig.3** shows that an increase in Schmidt number corresponds to a weaker solute diffusivity which allows a shallower penetration of solutal effect, as consequence, the concentration decreases with increase in Sc . It is observed in **Fig.4** that, an increase in the chemical absorption parameter (Ka) leads to increase in the temperature of the fluid and vice-versa, it is also noted that in the absence of chemical absorption ($Ka = 0$) the temperature reduces drastically, these is in excellent agreement with the work of Fetecau *et al.*[20].

In **Fig.5**, the effect of chemical reaction on velocity is shown when other parameters are considered as constants. It is noticed from the Figure that there is marked effect of increasing the value of chemical reaction parameter (Kr) on velocity profile in the boundary layer. It is highlighted that the velocity decreases with increase in the rate of chemical reaction, this is due to the fact that increase in chemical reaction rate leads to a fall in the momentum boundary layer. **Fig.6**, highlighted the effects of chemical absorption parameter on velocity

profile, it is observed that the increase in chemical absorption parameter leads to decrease in the velocity profile significantly and vice-versa. **Fig.7** depicts the effects of Solutal grashof number (Gr_c), it is described as the ratio of the species buoyancy force to the viscous hydrodynamic force. As solutal grashof number increases, the viscous hydrodynamic force decreases, as a result, the momentum boundary layer thickens and vice-versa. In **Fig.8**, it is observed that the fluid velocity decreases as the magnetic field parameter increases, this is due to the fact that, the application of transverse magnetic field to an electrically conducting fluid gives rise to resistive type of force called Lorentz force. This force has the tendency to slow down the motion of the fluid, consequently, the fluid velocity reduced significantly; this result is consistently agreed with that of Sheikholeslami and Gamji [5]. **Fig.9**, is prepared to show the influence of Schmidt number on Sherwood number versus chemical reaction parameter (Kr), an increase in Schmidt number decreases the Sherwood number in the interval $0 \leq Kr \leq 2$. It is evidence from **Fig.10** that, an increase in chemical absorption parameter (Ka) leads to decrease in the rate of heat transfer and vice-versa.

Also **Fig.11**, shows the effect of chemical reaction parameter on Nusselt number (Nu), it is observed from the figure that an increase in chemical reaction parameter decreases the rate of heat transfer and vice-versa, reverse trend is observed in **Fig.12**, as an increase in chemical reaction parameter decreases the rate of heat transfer.

However, **Fig.13** delicates effect of magnetic parameter on the skin friction coefficient, it is observed that increase in magnetic parameter decrease the skin friction coefficient (C_f), and vice-versa.

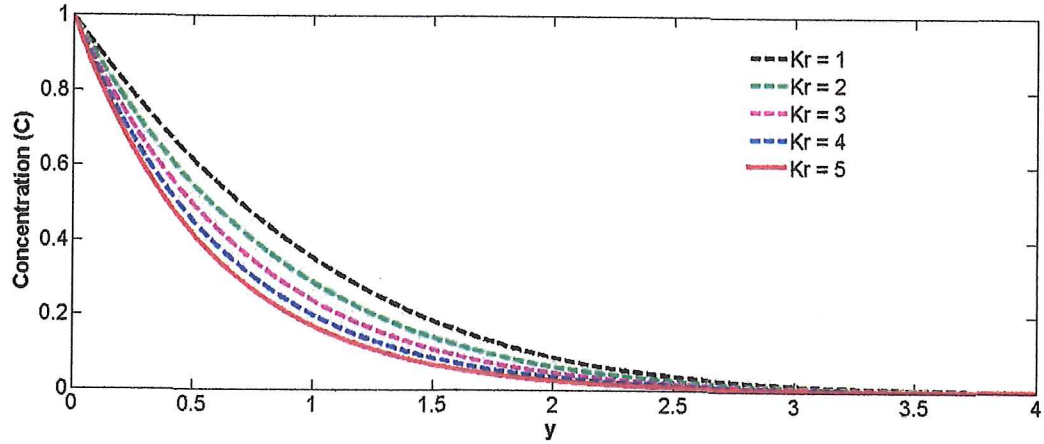


Fig.2 Effects of chemical reaction parameter (Kr) on concentration profile when $Sc = 0.6$, $t = 0.5$.

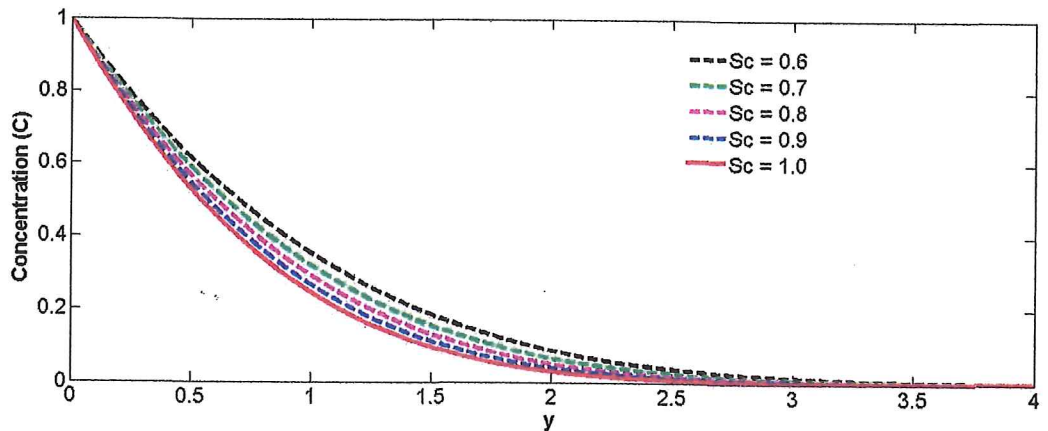


Fig.3 Effects of Schmidt number (Sc) on concentration profile when $Kr = 1$, $t = 0.5$.

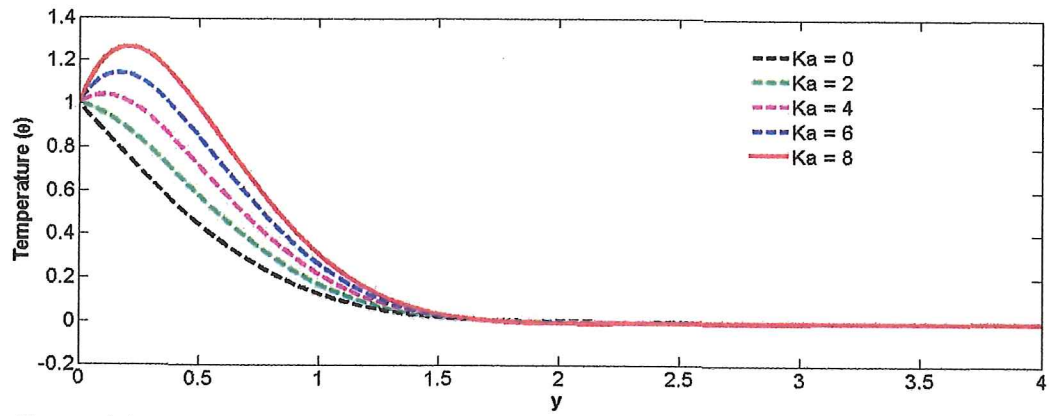


Fig.4 Effects of chemical absorption parameter (Ka) on temperature profile

when $Kr = 10$,

$$t = 0.5, R = 1, \varphi = 0.2, Pr = 6.2, Sc = 0.6.$$

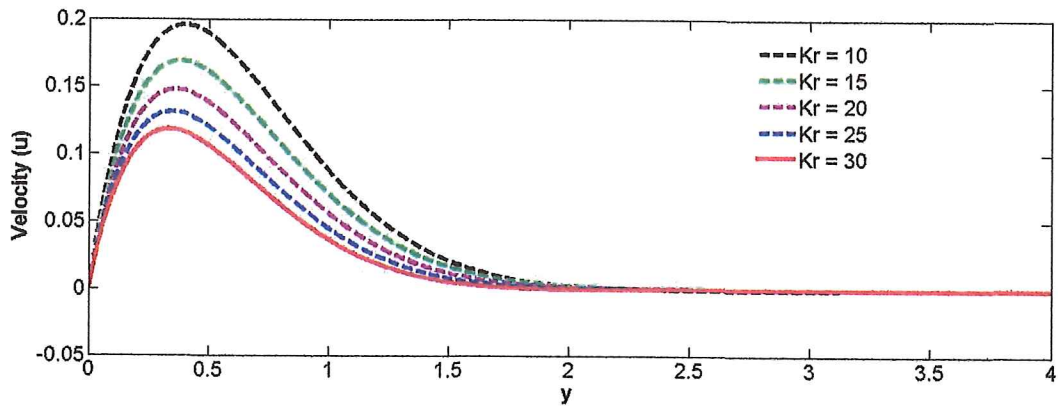


Fig.5 Effects of chemical reaction parameter (Kr) on velocity profile when $t = 0.5$,

$R = 1$

$$\varphi = 0.2, Pr = 6.2, Sc = 0.6, M = 0.1, Grc = 1, Grt = 0.1.$$

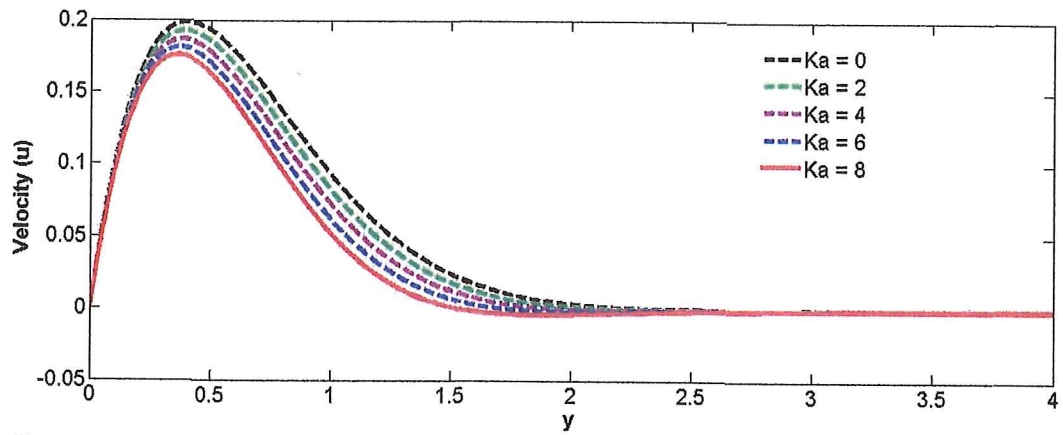


Fig.6 Effects of chemical absorption parameter (Ka) on velocity profile when

$t = 0.5, R = 1$

$\varphi = 0.2, Pr = 6.2, Sc = 0.6, M = 0.1, Grc = 1, Grt = 0.1, Kr = 10$

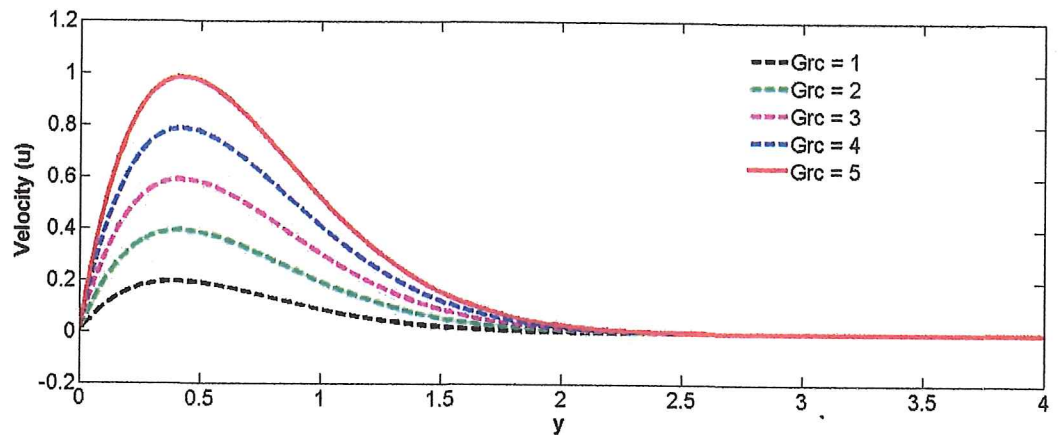


Fig.7 Effects of Solutal grashof number (Grc) on velocity profile when $Kr = 10,$

$t = 0.5, R = 1,$

$\varphi = 0.2, Pr = 6.2, Sc = 0.6, M = 0.1, Ka = 1, Grt = 0.1.$

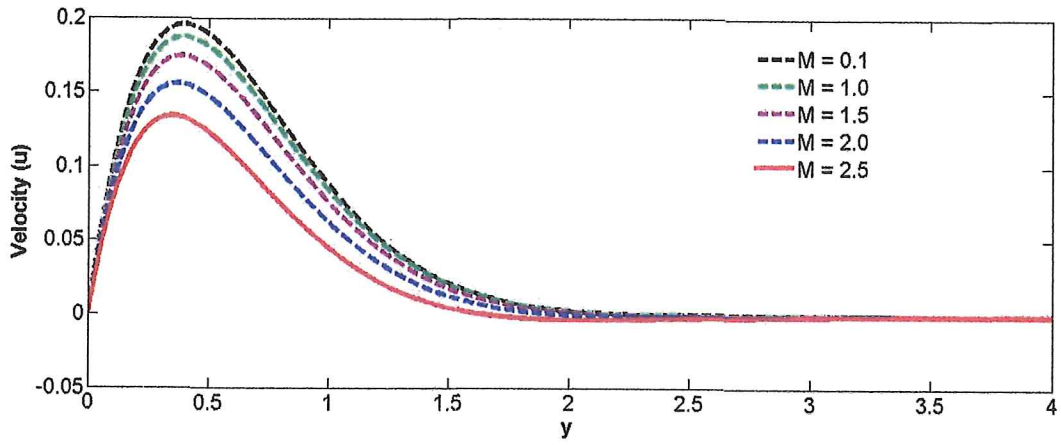


Fig.8 Effects of Magnetic parameter (M) on velocity profile when $Kr = 10, t = 0.5,$
 $R = 1,$

$$\varphi = 0.2, Pr = 6.2, Sc = 0.6, Ka = 1, Grc = 1, Grt = 0.1.$$

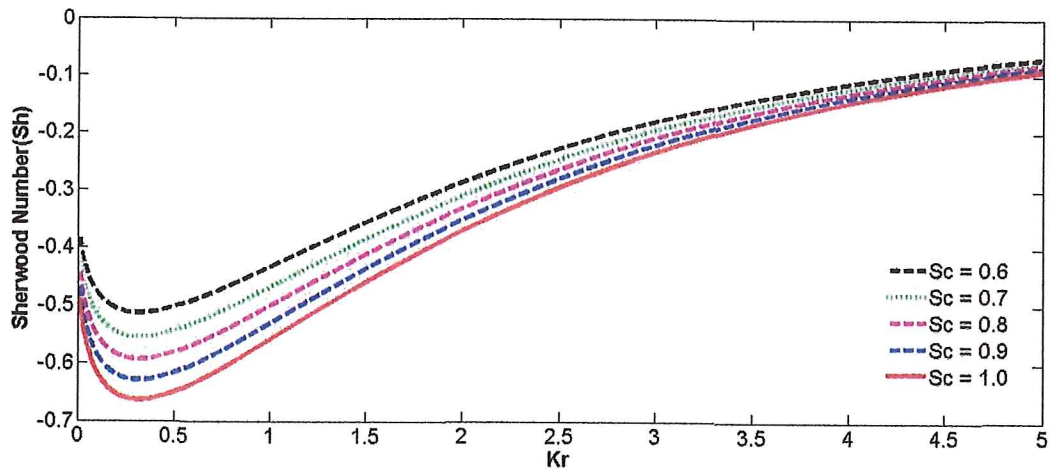


Fig.9 Effects of Schmidt number (Sc) on Sherwood number when $t = 0.5.$

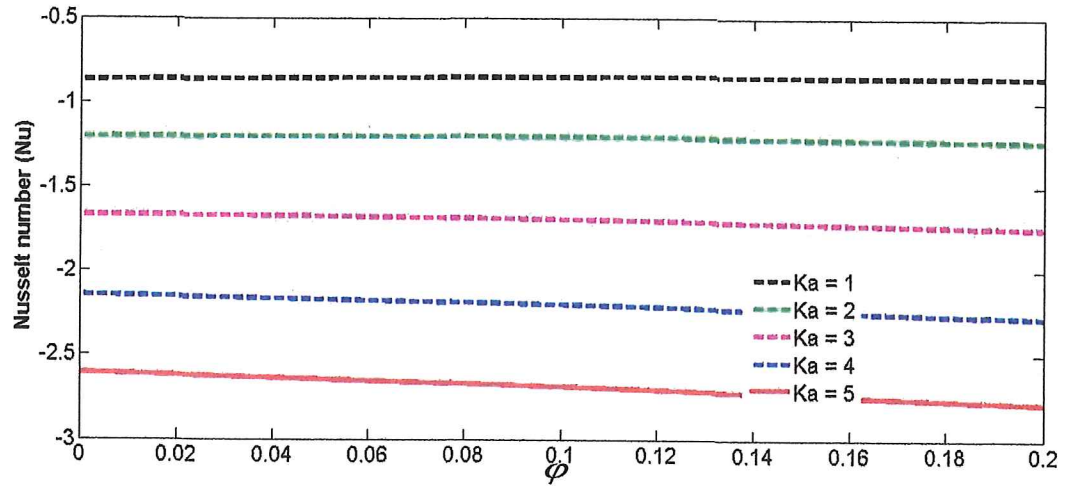


Fig.10 Effects of chemical absorption parameter (Ka) on Nusselt number when

$Kr = 10, t = 0.5$

$R = 1, \phi = 0.2, Pr = 6.2, Sc = 0.6$.

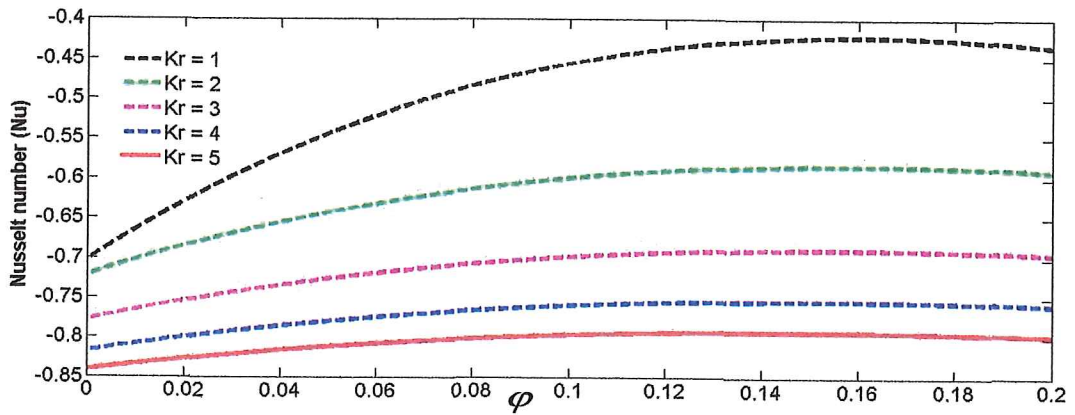


Fig.11 Effects of chemical reaction parameter (Kr) on Nusselt number when

$t = 0.5, R = 1, Sc = 0.6, Pr = 6.2, Ka = 1$.

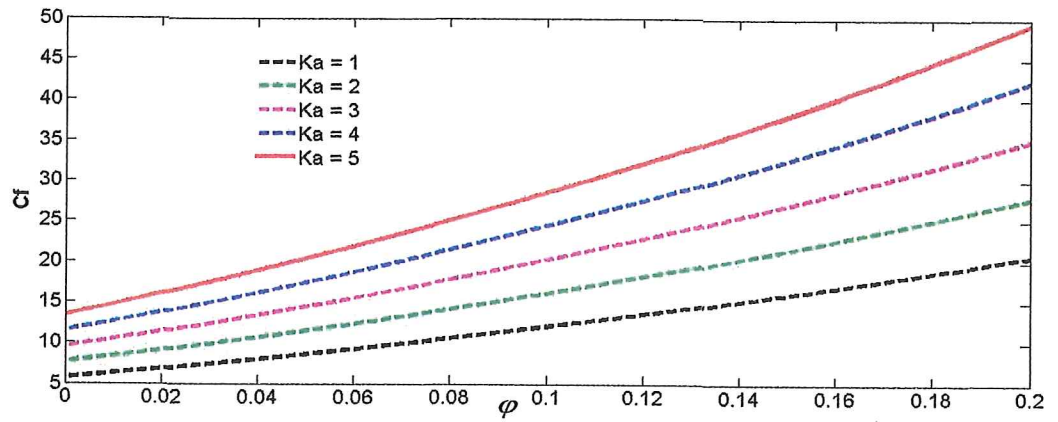


Fig.12 Effects of chemical absorption parameter (Ka) on Skin friction when $Kr = 10, t = 0.5, R = 1, Pr = 6.2, Sc = 0.6, Ka = 1, Grc = 1, Grt = 0.1$.

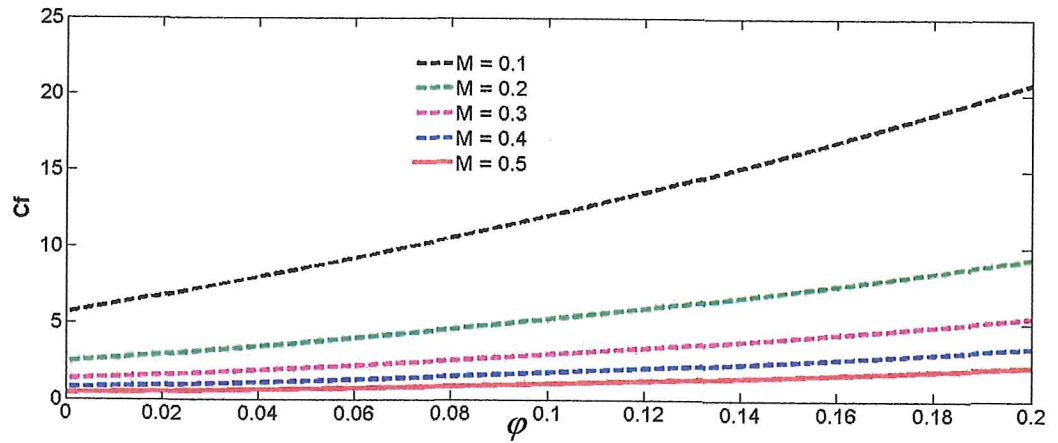


Fig.13 Effects of Magnetic parameter (M) on Skin friction profile when $Kr = 10, t = 0.5, R = 1, Pr = 6.2, Sc = 0.6, Ka = 1, Grc = 1, Grt = 0.1$.

4.0 Conclusion

The heat mass transfer of nanofluids flow with absorption in the presence of thermal radiation has been studied, the set of governing equations has been solved analytically using Laplace transform technique, the effects of pertinent parameters on the nanofluid concentration, temperature, velocity, rate of mass transfer, rate of heat transfer and skin friction are investigated and analyzed with the help of their graphical representations. Based on the results, the following conclusions are drawn:

- The presence of Chemical reaction reduces the concentration and velocity of the fluid.
- Chemical absorption parameter causes to increase the temperature of the fluid and causes to decrease the velocity of the fluid.
- Intensifying magnetic field strength stabilizes the velocity of the fluid.
- The influence of solutal grashof number and chemical absorption parameter are opposite on velocity field.
- As a result of chemical reaction and chemical absorption, the rate of the flow enhances.
- An increase in chemical reaction parameter decreases the rate of heat transfer of the fluid.

References

- [1] Wang, X.Q and Mujumdar, A.S.(2008).A review on nanofluids .part 1:theoretical and numerical investigations.*Brazilian Journal of Chemical Engineering*,**25(4)**,613-630.
- [2] Kakaç, S., and Pramuanjaroenkij, A. (2009). Review of convective heat transfer enhancement with nanofluids.*International Journal of Heat and Mass Transfer*, **52(13-14)**, 3187-3196.
- [3] Eapen, J., Rusconi, R., Piazza, R., and Yip, S. (2010). The classical nature of thermal conduction in nanofluids. *Journal of heat transfer*, **132(10)**, 102402.
- [4] Fan, J., and Wang, L. (2011). Review of heat conduction in nanofluids. *Journal of Heat Transfer*, **133(4)**, 040801.
- [5] Sheikholeslami, M., and Ganji, D. D. (2014). Magnetohydrodynamic flow in a permeable channel filled with nanofluid.*Scientia Iranica. Transaction B, Mechanical Engineering*, **21(1)**, 203.
- [6] Kuznetsov, A. V., and Nield, D. A. (2010). Natural convective boundary-layer flow of a nanofluid past a vertical plate.*International Journal of Thermal Sciences*, **49(2)**, 243-247.
- [7] Hamad, M. A. A., and Pop, I. (2011). Unsteady MHD free convection flow past a vertical permeable flat plate in a rotating frame of reference with constant heat source in a nanofluid.*Heat and mass transfer*, **47(12)**, 1517.

- [8] Turkyilmazoglu, M. (2012). Exact analytical solutions for heat and mass transfer of MHD slip flow in nanofluids. *Chemical Engineering Science*, **84**, 182-187.
- [9] Turkyilmazoglu, M., and Pop, I. (2013). Heat and mass transfer of unsteady natural convection flow of some nanofluids past a vertical infinite flat plate with radiation effect. *International Journal of Heat and Mass Transfer*, **59**, 167-171.
- [10] Das, K. (2014). Flow and heat transfer characteristics of nanofluids in a rotating frame. *Alexandria engineering journal*, **53(3)**, 757-766.
- [11] Sheikholeslami, M., Ganji, D. D., and Rashidi, M. M. (2015). Ferrofluid flow and heat transfer in a semi annulus enclosure in the presence of magnetic source considering thermal radiation. *Journal of the Taiwan Institute of Chemical Engineers*, **47**, 6-17.
- [12] Gireesha, B. J., Mahanthesh, B., and Gorla, R. S. R. (2014). Suspended particle effect on nanofluid boundary layer flow past a stretching surface. *Journal of nanofluids*, **3(3)**, 267-277.
- [13] Das, S., and Jana, R. N. (2015). Natural convective magneto-nanofluid flow and radiative heat transfer past a moving vertical plate. *Alexandria Engineering Journal*, **54(1)**, 55-64.
- [14] Gireesha, B. J., Mahanthesh, B., Shivakumara, I. S., and Eshwarappa, K. M. (2016). Melting heat transfer in boundary layer stagnation-point flow of nanofluid toward a stretching sheet with induced magnetic field. *Engineering Science and Technology, an International Journal*, **19(1)**, 313-321.

- [15] Mahdy, A., and ElShehabey, H. M. (2012). Uncertainties in physical property effects on viscous flow and heat transfer over a nonlinearly stretching sheet with nanofluids. *International Communications in Heat and Mass Transfer*, **39(5)**, 713-719.
- [16] Pal, D., and Talukdar, B. (2010). Perturbation analysis of unsteady magnetohydrodynamic convective heat and mass transfer in a boundary layer slip flow past a vertical permeable plate with thermal radiation and chemical reaction. *Communications in Nonlinear Science and Numerical Simulation*, **15(7)**, 1813-1830.
- [17] Chamkha, A. J. (2003). MHD flow of a uniformly stretched vertical permeable surface in the presence of heat generation/absorption and a chemical reaction. *International Communications in Heat and Mass Transfer*, **30(3)**, 413-422.
- [18] Uwanta, I. J., and Omokhuale, E. (2012). Viscoelastic fluid flow in a fixed plane with heat and mass transfer. *Research Journal of Mathematics and Statistics*, **4(3)**, 63-69.
- [19] Ali, F., Khan, I., and Shafie, S. (2013). Conjugate effects of heat and mass transfer on MHD free convection flow over an inclined plate embedded in a porous medium. *PloS one*, **8(6)**, e65223.
- [20] Fetecau, C., Vieru, D., and Azhar, W. A. (2017). Natural convection flow of fractional nanofluids over an isothermal vertical plate with thermal radiation. *Applied Sciences*, **7(3)**, 247.

[21] Tiwari,R.K.,and Das,M.K.(2007).Heat transfer augment in a two-sided Lid-driven DifferentiallyHeated square cavityUtilizing Nanofluids,*Int.J.Heat MassTransfer*,**50**,2002-2018.

[22] Oztoz,H.F.,and Abu-Nada,E.(2009).Numerical study of natural convection in partiallyheated rectangular enclosuresfilled with nanofluids,*Int.J.Heat Fluid Flow*,**29**,1326-1336.

APPENDICES

$$x_1 = \left(1 - \varphi + \varphi \frac{\rho_s}{\rho_f} \right),$$

$$x_2 = (1 - \varphi)^{2.5},$$

$$x_3 = \left(1 - \varphi + \varphi \frac{(\rho\beta)_s}{(\rho\beta)_f} \right),$$

$$x_4 = \left(1 + \frac{3(\sigma - 1)\varphi}{(\sigma + 2) - (\sigma - 1)\varphi} \right)$$

$$x_5 = \left(1 - \varphi + \varphi \frac{(\rho CP)_s}{(\rho CP)_f} \right),$$

$$x_6 = \frac{K_{nf}}{K_f},$$

$$a_1 = x_1 x_2,$$

$$a_2 = \frac{x_3}{x_1},$$

$$a_3 = \frac{a_2 G_{nc}}{G_n},$$

$$a_4 = \frac{x_4}{x_1},$$

$$a_5 = a_4 M^2,$$

$$a_6 = \frac{\text{Pr } x_5}{x_6 + R},$$

$$a_7 = \frac{Ka}{x_5}$$

$$V_1 = \frac{KrSc}{a_6 - Sc},$$

$$V_2 = \frac{a_6 a_7}{a_6 - Sc},$$

$$V_3 = \frac{a_1 a_2}{a_6 - a_1},$$

$$V_4 = \frac{a_1 a_5}{a_6 - a_1},$$

$$V_5 = \frac{a_6 a_1 a_2 a_7}{(a_6 - a_1)(a_6 - Sc)}$$

$$V_6 = \frac{a_6 a_1 a_2 a_7}{(a_6 - Sc)(a_1 - Sc)},$$

$$V_7 = \frac{a_1 a_5 - KrSc}{(a_1 - Sc)},$$

$$V_8 = \frac{a_1 a_4}{a_1 - Sc}.$$

$$b_1 = \frac{V_3}{V_4},$$

$$b_2 = \frac{V_5}{V_1 V_4},$$

$$b_3 = \frac{V_5}{(V_4 - V_1)V_4},$$

$$b_4 = \frac{V_5}{(V_1 - V_4)V_1},$$

$$b_5 = \frac{V_6}{(V_1 + V_7)V_7},$$

$$b_6 = \frac{V_6}{(V_1 + V_7)V_1},$$

$$b_7 = \frac{V_6}{V_1 V_7},$$

$$b_8 = \frac{V_8}{V_7},$$

$$b_9 = b_1 - b_3,$$

$$b_{10} = b_7 - b_1 - b_2 - b_8,$$

$$b_{11} = b_3 - b_1,$$

$$b_{12} = b_1 + b_2,$$

$$b_{13} = b_4 + b_6,$$

$$b_{14} = b_5 - b_8,$$

$$b_{15} = b_8 - b_7.$$

$$c_1 = V_1 + Kr,$$

$$c_2 = \frac{V_2}{V_1},$$

$$c_3 = V_4 + a_5,$$

$$c_4 = V_1 + a_5,$$

$$c_5 = -V_7 + Kr,$$

$$c_6 = -V_7 + a_5.$$

$$I_1 = \frac{1}{2} \left(\ell^{\gamma \sqrt{c_3 a_1}} \operatorname{erfc} \left(\frac{\gamma}{2} \sqrt{\frac{a_1}{t}} + \sqrt{c_3 t} \right) + \ell^{-\gamma \sqrt{c_3 a_1}} \operatorname{erfc} \left(\frac{\gamma}{2} \sqrt{\frac{a_1}{t}} - \sqrt{c_3 t} \right) \right)$$

$$I_2 = \frac{1}{2} \left(\ell^{\gamma \sqrt{a_1 a_5}} \operatorname{erfc} \left(\frac{\gamma}{2} \sqrt{\frac{a_1}{t}} + \sqrt{a_5 t} \right) + \ell^{-\gamma \sqrt{a_1 a_5}} \operatorname{erfc} \left(\frac{\gamma}{2} \sqrt{\frac{a_1}{t}} - \sqrt{a_5 t} \right) \right)$$

$$I_3 = \frac{1}{2} \left(\ell^{\gamma \sqrt{V_4 a_6}} \operatorname{erfc} \left(\frac{\gamma}{2} \sqrt{\frac{a_6}{t}} + \sqrt{V_4 t} \right) + \ell^{-\gamma \sqrt{V_4 a_6}} \operatorname{erfc} \left(\frac{\gamma}{2} \sqrt{\frac{a_6}{t}} - \sqrt{V_4 t} \right) \right)$$

$$I_4 = \operatorname{erfc} \left(\frac{\gamma}{2} \sqrt{\frac{a_6}{t}} \right)$$

$$I_5 = \frac{1}{2} \left(\ell^{\gamma \sqrt{V_1 a_6}} \operatorname{erfc} \left(\frac{\gamma}{2} \sqrt{\frac{a_6}{t}} + \sqrt{V_1 t} \right) + \ell^{-\gamma \sqrt{V_1 a_6}} \operatorname{erfc} \left(\frac{\gamma}{2} \sqrt{\frac{a_6}{t}} - \sqrt{V_1 t} \right) \right)$$

$$I_6 = \frac{1}{2} \left(\ell^{\gamma \sqrt{c_4 a_1}} \operatorname{erfc} \left(\frac{\gamma}{2} \sqrt{\frac{a_1}{t}} + \sqrt{c_4 t} \right) + \ell^{-\gamma \sqrt{c_4 a_1}} \operatorname{erfc} \left(\frac{\gamma}{2} \sqrt{\frac{a_1}{t}} - \sqrt{c_4 t} \right) \right)$$

$$I_7 = \frac{1}{2} \left(\ell^{\gamma \sqrt{c_5 S c}} \operatorname{erfc} \left(\frac{\gamma}{2} \sqrt{\frac{S c}{t}} + \sqrt{c_5 t} \right) + \ell^{-\gamma \sqrt{c_5 S c}} \operatorname{erfc} \left(\frac{\gamma}{2} \sqrt{\frac{S c}{t}} - \sqrt{c_5 t} \right) \right)$$

$$I_8 = \frac{1}{2} \left(\ell^{\gamma \sqrt{c_6 S c}} \operatorname{erfc} \left(\frac{\gamma}{2} \sqrt{\frac{S c}{t}} + \sqrt{c_6 t} \right) + \ell^{-\gamma \sqrt{c_6 S c}} \operatorname{erfc} \left(\frac{\gamma}{2} \sqrt{\frac{S c}{t}} - \sqrt{c_6 t} \right) \right)$$

$$I_9 = \frac{1}{2} \left(\ell^{\gamma \sqrt{K r S c}} \operatorname{erfc} \left(\frac{\gamma}{2} \sqrt{\frac{S c}{t}} + \sqrt{K r t} \right) + \ell^{-\gamma \sqrt{K r S c}} \operatorname{erfc} \left(\frac{\gamma}{2} \sqrt{\frac{S c}{t}} - \sqrt{K r t} \right) \right)$$

$$I_{10} = \frac{1}{2} \left(\ell^{\gamma \sqrt{c_6 a_1}} \operatorname{erfc} \left(\frac{\gamma}{2} \sqrt{\frac{a_1}{t}} + \sqrt{c_6 t} \right) + \ell^{-\gamma \sqrt{c_6 a_1}} \operatorname{erfc} \left(\frac{\gamma}{2} \sqrt{\frac{a_1}{t}} - \sqrt{c_6 t} \right) \right)$$

$$\left. \frac{\partial I_1}{\partial y} \right|_{y=0} = \sqrt{\frac{a_1}{\pi t}} \ell^{-c_3 t} + \sqrt{a_1 c_3} \operatorname{erfc}(\sqrt{c_3 t})$$

$$\left. \frac{\partial I_2}{\partial y} \right|_{y=0} = \sqrt{\frac{a_1}{\pi t}} \ell^{-a_5 t} + \sqrt{a_1 a_5} \operatorname{erfc}(\sqrt{a_5 t})$$

$$\left. \frac{\partial I_3}{\partial y} \right|_{y=0} = \sqrt{\frac{a_6}{\pi t}} \ell^{-V_4 t} + \sqrt{a_6 V_4} \operatorname{erfc}(\sqrt{V_4 t})$$

$$\left. \frac{\partial I_4}{\partial y} \right|_{y=0} = \sqrt{\frac{a_6}{\pi t}}$$

$$\left. \frac{\partial I_5}{\partial y} \right|_{y=0} = \sqrt{\frac{a_6}{\pi t}} e^{-V_2 t} + \sqrt{a_6 V_2} \operatorname{erfc}(\sqrt{V_2 t})$$

$$\left. \frac{\partial I_6}{\partial y} \right|_{y=0} = \sqrt{\frac{a_1}{\pi t}} e^{-c_4 t} + \sqrt{a_1 c_4} \operatorname{erfc}(\sqrt{c_4 t})$$

$$\left. \frac{\partial I_7}{\partial y} \right|_{y=0} = \sqrt{\frac{Sc}{\pi t}} e^{-c_5 t} + \sqrt{c_5 Sc} \operatorname{erfc}(\sqrt{c_5 t})$$

$$\left. \frac{\partial I_8}{\partial y} \right|_{y=0} = \sqrt{\frac{Sc}{\pi t}} e^{-c_6 t} + \sqrt{c_6 Sc} \operatorname{erfc}(\sqrt{c_6 t})$$

$$\left. \frac{\partial I_9}{\partial y} \right|_{y=0} = \sqrt{\frac{Sc}{\pi t}} e^{-Krt} + \sqrt{Krt Sc} \operatorname{erfc}(\sqrt{Krt})$$

$$\left. \frac{\partial I_{10}}{\partial y} \right|_{y=0} = \sqrt{\frac{a_1}{\pi t}} e^{-c_6 t} + \sqrt{c_6 a_1} \operatorname{erfc}(\sqrt{c_6 t})$$